Coulomb Formation Conservation Laws Using Differential Orbit Elements

Mischa Kim and Hanspeter Schaub

Simulated Reprint from

Proceedings of the Institution of Mechanical Engineers, Part G: Journal of Aerospace Engineering

Vol. 220, No. 5, July 2006, pp. 463–474

COULOMB FORMATION CONSERVATION LAWS USING DIFFERENTIAL ORBIT ELEMENTS

MISCHA KIM
Department of Aerospace Engineering
Embry-Riddle Aeronautical University
Prescott, AZ 86301, USA
e–mail: mischa.kim@erau.edu

and

HANSPETER SCHAUB
Department of Aerospace and Ocean Engineering
Virginia Polytechnic Institute and State University
Blacksburg, Virginia 24061, USA
e–mail: schaub@vt.edu

Abstract. Recently the concept of controlling the relative motion of spacecraft using electrostatic charging (Coulomb forces) has been proposed. For tight spacecraft formations with separation distances ranging from 10–100 meters, the Coulomb forces between the spacecraft can be exploited to provide an extremely fuel and power efficient means of propulsion. As the charge of a single craft is varied, the relative motion of the entire formation is affected. The Coulomb force vector a craft experiences is restricted to be directed along the relative position vectors, which results in constraints being imposed on how the Coulomb force can be used to control a formation. This paper investigates how the conservation of angular momentum and the formation center of mass limits the types of relative orbits that can be controlled. Considering the spacecraft formation to be a system of N particles, the formation internal Coulomb force can not change the inertial system angular momentum vector. The center of mass definition and angular momentum constraint are expressed using differential orbit elements to describe the relative motion. Both Cartesian and orbit element formation center of mass are discussed. First-order transformations to the nonlinear solutions are presented. Their accuracy is evaluated both analytically and using numerical simulations. The orbit element center of mass of the charged spacecraft formation can be approximated to be Keplerian for charge feedback laws which are proportional to the orbit element tracking errors.

Key words: Coulomb satellite formations, differential orbital elements, formation center of mass, orbit element center of mass.

NOMENCLATURE

a	semimajor axis
$\mathbf{A}$	sensitivity matrix
α	angle
$\mathbf{B}$	control influence matrix
c	root mean square deviation approximation constant
$\mathbf{C}$	general rotation matrix
$\mathbf{C}_k$	single-axis (k) rotation matrix
δ_u	"small" state
e	eccentricity
ϵ	relative deviation error
f	true anomaly
f_u	true anomaly phase angle for in-plane relative motion
γ	root mean square deviation ratio
$\mathbf{\Gamma}$	orbit elements to Cartesian coordinates mapping function
h	total specific angular momentum magnitude
$\boldsymbol{h}$	total specific angular momentum
$\mathcal{H}$	Hill frame
$\boldsymbol{H}$	total angular momentum
i	inclination
$\hat{\boldsymbol{\imath}}_h$	orbit normal vector
I_{sp}	specific impulse
k_c	Coulomb constant
λ_d	Debye length
m	spacecraft mass
M	total spacecraft formation mass
M_0	initial mean anomaly
μ	gravitational parameter
η	eccentricity measure
$\boldsymbol{\xi}$	position vector in orbital frame
$\mathcal{O}$	order symbol
$\boldsymbol{\mathfrak{oe}}$	classical orbit elements
ω	argument of periapsis
Ω	argument of the ascending node
p	semilatus rectum
$\boldsymbol{p}$	linear momentum
q	spacecraft charge
$\boldsymbol{r}$	relative spacecraft position vector
$\boldsymbol{R}$	absolute spacecraft position vector
ρ	orbital radius
$\mathbf{S}$	singular values matrix
t	time
θ_w	true latitude phase angle for out-of-plane relative motion
u	non-dimensional x-coordinate in Hill frame
$\boldsymbol{u}$	control acceleration vector
$\mathbf{U}$	left singular vectors matrix
v	non-dimensional y-coordinate in Hill frame
$\mathbf{V}$	right singular vectors matrix
w	non-dimensional z-coordinate in Hill frame
x	x-coordinate in Hill frame

$\boldsymbol{X}$	state vector
y	y-coordinate in Hill frame
z	z-coordinate in Hill frame
⏢	orbit element center of mass
⌾	cartesian center of mass

1. Introduction

Spacecraft formation flying control is a challenging research thrust requiring a fundamental understanding of both orbital mechanics and control theory. Typically, the amount of propellant aboard a craft is limited. Nevertheless, even with a carefully chosen relative orbit geometry, the control system typically needs to perform minor orbit corrections periodically to maintain the formation. Typical spacecraft interferometry missions, for example, consider separation distances ranging from hundreds of meters to multiple kilometers. Large baselines are used to provide a highly accurate sensing of a narrow field of view. The forces required for a continuous thrust propulsion system to maintain a relative orbit are of the order of mN or less. Pulsed-Plasma Thrusters (PPTs) and other ion engines are considered as the primary relative navigation propulsion method. The thrust is achieved by expelling charged ions at a very high velocity. To achieve high escape velocities, relatively large amounts of electrical power must be provided. Because exhaust plumes contain toxic chemicals that could damage another spacecraft or its sensors, care must be taken that the ion engine exhaust does not hit another craft. For formations with relative separations in the order of kilometers, the exhaust issue is not of concern.

Consider a tight formation to be defined as having spacecraft separation distances ranging between 10 and 100 meters. Such clusters could be used to perform high accuracy, very wide field of view missions at Geostationary Orbits (GEO). For example, 20-30 meter formations at GEO could observe the entire hemisphere with a meter level resolution with infinite dwell time. Alternatively, tight formations could be used to measure local gradients of magnetic or gravitational fields. Yet another application exploits the Coulomb forces to navigate a sensor about a larger spacecraft. In all of these scenarios, the ion engine exhaust plume issue is one of the primary mission concerns. However, with all craft flying in close proximity, collision avoidance and – in particular – fuel expenditure to perform the greatly increased number of relative orbit corrections are of major concern. The analysis provided in reference [1] use electrostatic charging as a means to perform relative orbit control. It was found that mN levels of thrust could be achieved between the vehicles with typical power requirements of < 1 Watt. Calculated I_{sp} fuel efficiencies were as high as 10^{10}–10^{13} seconds, rendering this mode of propulsion essentially propellant less. Measured spacecraft charging data obtained by the SCATHA GEO mission in 1979 verified that a craft can charge to high voltages in low space plasma environments such as GEO [2]. More recently, the CLUSTERS mission demonstrated the feasibility to control the spacecraft charge and maintain a near-zero voltage level [3]. Note that Coulomb force control is only effective for relatively tight formation/proximity flying scenarios of 10–100 meters due to the $1/r^2$ behavior of the Coulomb electrostatic force magnitude, r being the spacecraft separation distance. For minimum separation distances larger than that, the required spacecraft charging levels simply become impractical due to differential charging issues. Additionally, Coulomb force effectiveness is diminished in a space plasma environment. The reduced effectiveness is measured through the Debye length, which indicates the exponential decay e^{-r/λ_d} of the electrostatic field strength [4, 5]. Because λ_d is in the order of centimeter for Low Earth Orbits (LEO), the Coulomb satellite concept is not practical at low altitudes. However, at GEO it was found that λ_d values are in the order of 100–1000 meters [1], making Coulomb formation flying (CFF) feasible at higher altitudes.

References [1, 6] discuss interesting steady-state solutions which exist for the charged relative orbit equations of motion. The authors show how such charged formations are able to establish fixed relative positions as seen by the rotating Hill coordinate frame. As a result the individual spacecraft can be shown to perform non-Keplerian orbits to maintain their formation position. Both in-plane and general three-dimensional steady-state equilibrium conditions were found. However, none of these formation shapes were found to be stable. Nonlinear charging control laws were

investigated for a two-satellite formation in reference [7], and for a larger cluster of Coulomb satellites in reference [8]. An orbit element difference approach was used to describe and control the relative motion. However, in these control developments, only general stability properties were provided. Asymptotic convergence was only discussed for algorithms controlling semi-major axis exclusively. For example, it is intuitive that the inter spacecraft Coulomb forces cannot be used to change a relative orbit from being an in-plane formation to having out-of-plane components.

Because Coulomb force control inherently only allows for relative motion control (spacecraft are pushing and pulling off each other), it is natural to describe relative motion of a Coulomb formation with respect to the formation center of mass. The single-craft control strategies developed in references [7, 8] identify the formation chief position as the formation center of mass. Furthermore, these papers assume the Coulomb formation chief to be moving in a Keplerian, unperturbed orbit. As shown in reference [9], these assumptions are valid approximations and particularly feasible for small formations using Coulomb thrusting. The analysis in reference [9] examines relative motion constraints of Coulomb formations for satellite motion described using either inertial or formation-center-of-mass relative position vectors.

This paper investigates how conservation of inertial angular momentum and the formation center of mass definition constrain the evolution of Coulomb formations if the relative motion is expressed using differential orbit elements. The formation center of mass definition is a simple linear relationship only when using Cartesian coordinates. On the other hand, the Cartesian center of mass definition becomes a nonlinear function using an orbit elements system description. Similarly, the precise momentum constraint using orbit element differences is a complex function. First order approximations are introduced for these transformations and their accuracy is discussed both analytically and through numerical illustrations. In particular, the concept of an orbit element based formation center of mass is introduced and compared to the classical Cartesian formation center of mass. When controlling Coulomb formations, it is more meaningful to describe the formation with respect to the orbit element center of mass versus the Cartesian formation center of mass. The presented first order orbit element constraints on Coulomb formations can be used in control analysis research to investigate convergence and feasible relative motion.

2. Problem Statement

Rather than using traditional Cartesian coordinates with respect to the rotating Hill frame, classical orbit elements $\boldsymbol{oe} = \{a, e, i, \Omega, \omega, M_0\}$ are used to describe the satellite motion. Note that semi-major axis a, eccentricity e, orbit inclination angle i, ascending node angle Ω and argument of periapses ω, as well as initial mean anomaly M_0, are constants of the unperturbed orbital motion (Keplerian motion case). To describe the satellite motion relative to the formation center of mass, differences in orbit elements $\delta\boldsymbol{oe} = \boldsymbol{oe} - \boldsymbol{oe}_c$ are used with respect to the formation center of mass orbit elements $\boldsymbol{oe}_c$. For unperturbed, uncontrolled relative motion, these differenced elements are constants.

It is convenient to describe Coulomb formations relative to the formation center of mass position vector $\boldsymbol{R}_c$. Because the electrostatic Coulomb force is a formation-internal force, the control can not change the formation inertial angular momentum. If $\boldsymbol{h}_i$ is the angular momentum per unit mass of the i^{th} satellite, then the formation inertial angular momentum

$$\boldsymbol{h} = \sum_{i=1}^{N} \boldsymbol{h}_i \tag{1}$$

must be a constant of motion, where N is the total number of spacecraft in the formation. This conservation law provides three integrals of motion of the charged relative motion dynamics. As pointed out before, the conservation of angular momentum is readily expressed using either inertial Cartesian position and velocity vectors $(\boldsymbol{R}_i, \dot{\boldsymbol{R}}_i)$ or inertial orbit elements $\boldsymbol{oe}$. However, the momentum constraint, as well as the formation center of mass definition, are more complex if relative position coordinates $\delta\boldsymbol{oe}$ are employed. Of interest are analytic approximations of the momentum and center of mass expressions using orbit element differences. While momentum conservation is specific to the study of Coulomb formations, the center of mass discussion is applicable to general spacecraft formations.

3. Center of Mass Definition

Let us first investigate the formation center of mass definition using differenced orbit elements. The inertial position and velocity vectors of the formation center of mass are traditionally defined using inertial Cartesian position and velocity vectors as

$$\boldsymbol{R}_c = \frac{1}{M}\sum_{i=1}^{N} m_i \boldsymbol{R}_i \tag{2}$$

$$\dot{\boldsymbol{R}}_c = \frac{1}{M}\sum_{i=1}^{N} m_i \dot{\boldsymbol{R}}_i \tag{3}$$

where $M = \sum_{i=1}^{N} m_i$ is the total formation mass. Eq. (2) defines the true formation Cartesian center of mass position vector. Later on, approximate solutions are compared to the classical formulation in Eq. (2). Using relative position vectors $\boldsymbol{r}_i = \boldsymbol{R}_i - \boldsymbol{R}_c$ with respect to the formation center of mass, Eq. (2) can be rewritten as

$$\sum_{i=1}^{N} m_i \, \boldsymbol{r}_i = \boldsymbol{0} \tag{4}$$

Note that Eq. (4) is a vector equation and must hold for any coordinate frame choice to express the vector components. Further the center of mass definition in Eq. (4) is equivalent to considering the relative linear momentum $\boldsymbol{p} = \sum_{i=1}^{N} m_i \dot{\boldsymbol{r}}$ to be an integral of motion. Let $\boldsymbol{r}_i$ vector components be expressed in the chief Local-Vertical-Local-Horizontal (LVLH) or Hill frame $\mathcal{H}$ as [10]

$${}^{\mathcal{H}}\boldsymbol{r}_i = \begin{pmatrix} x_i \\ y_i \\ z_i \end{pmatrix} \tag{5}$$

Next, let the non-dimensional relative position coordinates be defined through

$$u_i = \frac{x_i}{R_c} \qquad v_i = \frac{y_i}{R_c} \qquad w_i = \frac{z_i}{R_c} \tag{6}$$

Note that the formation center of mass radius R_c is time varying in general (elliptic orbits). An equivalent expression for the center of mass condition in Eq. (4) is expressed using (u, v, w) as

$$\sum_{i=1}^{N} m_i u_i = \sum_{i=1}^{N} m_i v_i = \sum_{i=1}^{N} m_i w_i = 0 \tag{7}$$

If the relative motion is expressed using Cartesian coordinates, as is commonly done when using the Clohessy-Wiltshire-Hill equations [10, 11, 12], center of mass definitions in either Eq. (2) or (7) could be used directly. However, if the relative motion is expressed using orbit element differences, the center of mass conditions are not obvious, especially if the chief orbit is allowed to be highly eccentric.

For the subsequent analysis the following notational short hand is used: orbit elements without subscripts are implied to denote the formation chief or center of mass. To find approximate first order center of mass conditions using orbit element differences, we first present a direct approach using the nonlinear map between Cartesian coordinates and orbital elements. Subsequently, we outline an alternative derivation using a relative motion description presented in references [13, 14].

Let $\boldsymbol{\Gamma} : \mathbb{R}^6 \to \mathbb{R}^6$ be the nonlinear mapping that transforms orbital elements into Cartesian orbit position coordinates, that is,

$$\boldsymbol{X} = \boldsymbol{\Gamma}(\boldsymbol{\alpha e}) \,, \qquad \text{where} \qquad \boldsymbol{X} \triangleq (\boldsymbol{R}, \dot{\boldsymbol{R}}) \tag{8}$$

Using the formation center of mass definition and expanding the resulting orbital element expressions into a Taylor series about the center of mass, we find that

$$\sum_{i=1}^{N} m_i(\boldsymbol{X}_i - \boldsymbol{X}_c) \equiv \sum_{i=1}^{N} m_i(\boldsymbol{\Gamma}(\boldsymbol{\alpha e}_i) - \boldsymbol{\Gamma}(\boldsymbol{\alpha e}_c)) = \sum_{i=1}^{N} m_i \mathbf{A}_c \delta\boldsymbol{\alpha e}_i + \mathcal{O}\big(\delta\alpha_i^2\big) = \mathbf{0} \tag{9}$$

The time-dependent sensitivity matrix $\mathbf{A}_c = (\partial/\partial\boldsymbol{\alpha e})\,\boldsymbol{\Gamma}(\boldsymbol{\alpha e}_i)|_c$ is evaluated at the formation center of mass and is therefore equal for all spacecraft. As a result we can pull $\mathbf{A}_c$ in front of the summation sign to obtain

$$\mathbf{A}_c \sum_{i=1}^{N} m_i \delta\boldsymbol{\alpha e}_i + \mathcal{O}\big(\delta\alpha_i^2\big) = \mathbf{0} \qquad \text{or} \qquad \sum_{i=1}^{N} m_i \delta\boldsymbol{\alpha e}_i = \mathcal{O}\big(\delta\alpha_i^2\big) \;\; \textit{iff} \;\; \det(\mathbf{A}_c) \neq 0 \tag{10}$$

Since the rank of a map is the rank of its differential, $\text{rank}(\boldsymbol{\Gamma}) = \text{rank}(\mathbf{A}_c)$. Considering only chief orbit element values that are not singular, $\det(\mathbf{A}_c) \neq 0$ and as a result the matrix $\mathbf{A}_c$ is invertible. The expression on the right-hand side of Eq. (10) is therefore accurate to second order. Equivalent first order classical orbit element difference expressions are summarized in the form of scalar equations as

$$\sum_{i=1}^{N} m_i\, \delta a_i = 0 \qquad \sum_{i=1}^{N} m_i\, \delta e_i = 0 \qquad \sum_{i=1}^{N} m_i\, \delta i_i = 0 \tag{11a}$$

$$\sum_{i=1}^{N} m_i\, \delta\Omega_i = 0 \qquad \sum_{i=1}^{N} m_i\, \delta\omega_i = 0 \qquad \sum_{i=1}^{N} m_i\, \delta M_i = 0 \tag{11b}$$

Note that Eqs. (11) are only first order approximations of the formation center of mass definition. While both the Cartesian coordinate center of mass definition in Eq. (2) and (4) are rigorously

true, the above orbit element difference conditions are first order approximations where we assume that the orbit element differences are small compared to the chief orbit elements. The result, that the mass-averaged sum of all relative orbit element differences must equal zero, is equivalent to the Cartesian version in Eq. (4).

Using small classical orbit element differences, non-dimensional (u, v, w) motion equations of each satellite can be written as [14]

$$u_i = \frac{\delta a_i}{a} - \frac{e\,\delta e_i}{2\eta^2} + \frac{1}{\eta^2}\delta_{u_i}\cos\left(f - f_{u_i}\right) + \frac{e}{2\eta^2}\delta_{u_i}\cos\left(2f - f_{u_i}\right) + \mathcal{O}(\delta\alpha e^2) \tag{12}$$

$$\begin{aligned} v_i = {} & \left(\left(1 + \frac{e^2}{2}\right)\frac{\delta M_i}{\eta^2} + \delta\omega_i + \cos i\,\delta\Omega_i\right) - 2\frac{\delta_{u_i}}{\eta^2}\sin\left(f - f_{u_i}\right) + \mathcal{O}(\delta\alpha e^2) \\ & - \frac{\delta_{u_i}}{\eta^2}\frac{e}{2}\sin\left(2f - f_{u_i}\right) \end{aligned} \tag{13}$$

$$w_i = \sqrt{\delta i_i^2 + \sin^2 i\,\delta\Omega_i^2}\cos\left(\theta - \theta_{w_i}\right) + \mathcal{O}(\delta\alpha e^2) \tag{14}$$

where

$$\delta_{u_i} = \sqrt{\frac{e^2\,\delta M_i^2}{\eta^2} + \delta e_i^2} \tag{15}$$

$$f_{u_i} = \tan^{-1}\left(\frac{e\,\delta M_i}{-\eta\delta e_i}\right) \tag{16}$$

$$\theta_{w_i} = \tan^{-1}\left(\frac{\delta i_i}{-\sin i\,\delta\Omega}\right) \tag{17}$$

This relative motion description is convenient for the current discussion because it provides a direct description of the general relative motion in terms of secular offsets and repeating trigonometric terms using orbit element differences. Contrary to the analytical solution of the Clohessy-Wiltshire-Hill equations, the first order relative motion solution is valid for both circular and elliptic chief motions.

Substituting Eqs. (12–14) into Eqs. (7) the (u, v, w) center of mass conditions are satisfied by requiring sums of the constant terms, terms depending on $\cos(f - f_{u_i})$, terms depending on $\cos(2f - f_{u_i})$, terms depending on $\sin(f - f_{u_i})$, and terms depending on $\sin(2f - f_{u_i})$ of Eqs. (12–14) to vanish independently. With some modest amount of algebra one ultimately obtains the same first order approximations of the formation center of mass as presented in Eqs. (11). This longer, but insightful approach to Eq. (11) is shown in full in Reference [15].

For the sake of clarity, we refer to the mass-averaged orbit element difference location as the Orbit Element center of mass (OECM ⏢). While not equal to the Cartesian center of mass (CCM ⊕), the OECM is of value when describing and controlling formations. Consider a simple leader- follower 2-satellite formation as illustrated in Figure 1, where the actual Cartesian center of mass would rotate at the same period as the satellites while having a smaller semi-major axis. For the more general elliptic inertial orbit case shown in Figure 1, the CCM clearly does not perform a Keplerian orbit motion [9]. Computing inertial formation center of mass position and velocity vectors $(\boldsymbol{R}_c, \dot{\boldsymbol{R}}_c)$, and translating these coordinates into equivalent orbit elements, we find that Keplerian motion predicts the center of mass to move faster than the satellites. Considering a control law that defines tracking errors with respect to the true formation Cartesian center of mass, the satellites are controlled with respect to a chief location which has a slightly different orbit period. In contrast, if the OECM

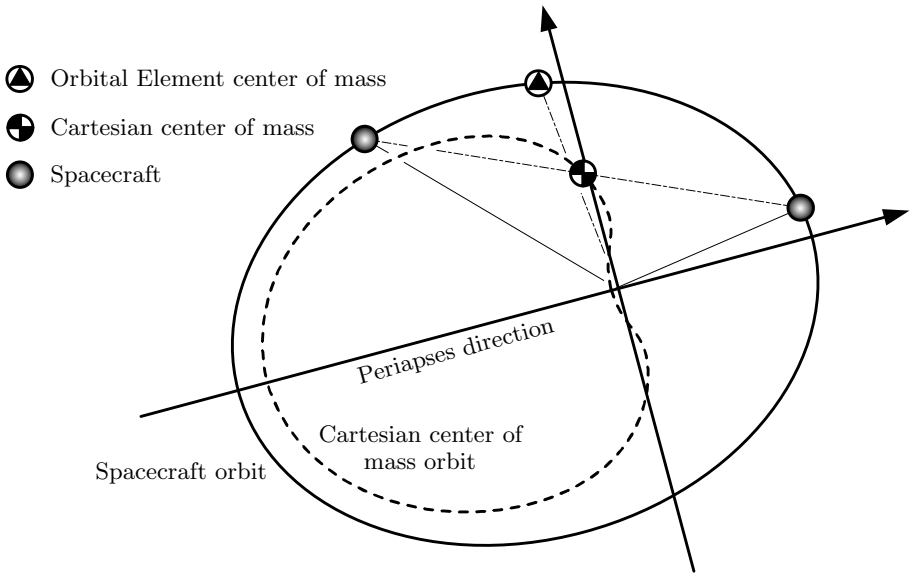

Figure 1. Cartesian center of mass versus Orbital Element center of mass locations for a formation of two largely separated spacecraft.

is computed using Eq. (11) for the leader-follower example, the OECM has the same semi-major axis as the other two satellites. Both satellites and center of mass travel at the same orbital rate assuming Keplerian motion. Thus, the OECM does indeed evolve in a Keplerian manner. Note that the differences between the Cartesian and orbit element center of mass locations are very small. A detailed error analysis follows in a later section. Thus, for orbit element difference based control strategies, it is advantageous to define and control the formation relative to the formation OECM. Because this location is Keplerian, its orbit elements $\boldsymbol{\alpha e}_{\rm OECM}$ will be constant.

Constraints in Eq. (11) on the motion of Coulomb formations are useful when analyzing orbit element based feedback control laws. For example, for the dual-craft formation discussed in [7], if $\delta a_1 \to 0$, the center of mass definition in Eq. (11) immediately implies that $\delta a_2 \to 0$, as well. In other words, for the 2-satellite system, showing convergence of one satellite is equivalent to showing convergence of the entire system.

4. Angular Momentum

As pointed out before, the inertial angular momentum vector $\boldsymbol{H}$ is a constant of motion for the formation because Coulomb forces are internal forces of the spacecraft formation [9]. Let $\boldsymbol{R}_i$ be the $i^{\rm th}$ inertial spacecraft position vector and m_i be the associated constant spacecraft mass. The spacecraft cluster is assumed to contain N craft. The total formation angular momentum is then expressed as [10]

$$\boldsymbol{H} = \sum_{i=1}^{N} \boldsymbol{H}_i = \sum_{i=1}^{N} m_i \boldsymbol{R}_i \times \dot{\boldsymbol{R}}_i = \sum_{i=1}^{N} m_i \boldsymbol{h}_i \tag{18}$$

where $\boldsymbol{h}_i = h_i \hat{\boldsymbol{\imath}}_{h_i}$ is the massless momentum vector and derivatives taken here are inertial time derivatives. Note that h_i can be expressed in terms of the semi-major axis a_i and the eccentricity measure $\eta_i = \sqrt{1-e_i^2}$ as

$$h_i = \sqrt{\mu a_i}\eta_i \tag{19}$$

The orbit normal vector is obtained as [10]

$$\hat{\boldsymbol{\imath}}_{h_i} = \begin{pmatrix} \sin i_i \sin\Omega_i \\ -\sin i_i \cos\Omega_i \\ \cos i_i \end{pmatrix} \tag{20}$$

where the vector components are taken with respect to an inertial frame $\mathcal{N}$. Using Eqs. (19) and (20), the total inertial Coulomb formation angular momentum vector can be written as

$$\boldsymbol{H}(\boldsymbol{\alpha e}) = \sum_{i=1}^{N} m_i \sqrt{\mu a_i}\eta_i \begin{pmatrix} \sin i_i \sin\Omega_i \\ -\sin i_i \cos\Omega_i \\ \cos i_i \end{pmatrix} \tag{21}$$

If inertial orbit elements are used instead of orbit element differences to describe the satellite motion, then Eq. (21) provides the full nonlinear formation angular momentum relationship. Because $\boldsymbol{H}$ is constant, Eq. (21) provides three momentum constraints on the Coulomb relative motion. Note that so far no approximations have been introduced to the momentum constraints.

Using the OECM location, the inertial angular momentum of the Orbital Element center of mass is, according to Eq. (21), $\boldsymbol{H}_{\text{OECM}} = \boldsymbol{H}(\boldsymbol{\alpha e})|_{\text{OECM}}$. Because the relative motion is expressed using orbit element differences, it is desirable to express the law of momentum conservation $\boldsymbol{H}(t) = \boldsymbol{H}(t_0)$ in terms of orbit element differences, as well. Rewriting the formation angular momentum in terms of orbit element differences, we expand $\boldsymbol{H}$ into a Taylor series about the OECM orbital elements to obtain:

$$\begin{aligned} \boldsymbol{H} &= \boldsymbol{H}_{\text{OECM}} + \sum_{i=1}^{N} \left.\frac{\partial \boldsymbol{h}_i}{\partial \boldsymbol{\alpha e}_i}\right|_{\text{OECM}} m_i\, \delta\boldsymbol{\alpha e}_i + \mathcal{O}\big(\delta\alpha e_i^2\big) \\ &= \boldsymbol{H}_{\text{OECM}} + \left(\left.\frac{\partial \boldsymbol{h}}{\partial \boldsymbol{\alpha e}}\right|_{\text{OECM}}\right) \sum_{i=1}^{N} m_i\, \delta\boldsymbol{\alpha e}_i + \mathcal{O}\big(\delta\alpha e_i^2\big) \\ &= \boldsymbol{H}_{\text{OECM}} + \mathcal{O}\big(\delta\alpha e_i^2\big) \end{aligned} \tag{22}$$

In Eq. (22) corresponding first-order derivatives of the massless momentum vectors $\boldsymbol{h}_i$ are evaluated at the common OECM and are therefore equal for all spacecraft. Pulling the derivatives in front of the summation sign and using Eqs. (10) we find the angular momentum of the OECM to be a second order accurate approximation of the constant formation momentum vector $\boldsymbol{H}$. In other words, the total formation inertial angular momentum vector $\boldsymbol{H}$ is not equal to the OECM angular momentum $\boldsymbol{H}_{\text{OECM}}$ in general. However, if relative spacecraft distances are "small"[†] compared to the inertial chief orbit radius, then $\boldsymbol{H}_{\text{OECM}}$ is reasonably close to the constant total formation inertial angular momentum, that is, $\boldsymbol{H}_{\text{OECM}} \approx \boldsymbol{H}$.

The next question is, what are the three momentum constraint equations in terms of $\delta\boldsymbol{\alpha e}_i$? We point out that Eq. (22) does not yield any linear $\delta\boldsymbol{\alpha e}$ terms. The answer is that the three momentum constraints in terms of $\delta\boldsymbol{\alpha e}_i$ are inherently satisfied if the formation center of mass

[†]We quantify the term "small" in section 5.1 of this paper.

condition $\sum_{i=1}^{N} m_i \delta\boldsymbol{\alpha e}_i = 0$ is satisfied. Thus, to first order, the six conditions in Eq. (11) include both the three center of mass and three momentum constraints. Expressing the relative motion using the orbit element differences $\delta\boldsymbol{\alpha e}_i$, we must assure that

$$\sum_{i=1}^{N} m_i \delta\boldsymbol{\alpha e}_i = 0 \tag{23}$$

is true to satisfy all six combined center of mass and momentum CFF constraints of the center of mass-relative formation description using orbit element differences. In case the true nonlinear constraints are to be used instead of the first-order approximation, then the center of mass constraint in Eq. (4) and inertial momentum constraint in Eq. (21) must be satisfied. The first-order approximation provides a much more convenient form for analysis of feasible relative motion dynamics or charged relative motion control.

5. Center of Mass Definitions Error Analysis

5.1. First Order Momentum Expression

As pointed out in a previous section, it proves advantageous for control analysis to define the center of mass of CFF using orbital elements and orbital element differences. Note that Eqs. (11) specify the formation center of mass location to first order only. A more general nonlinear analysis shows how center of mass approximations in the orbital element space map into actual position and velocity errors in inertial space.

The coordinates transformations $\boldsymbol{R}(\boldsymbol{\alpha e})$ and $\dot{\boldsymbol{R}}(\boldsymbol{\alpha e})$ of mapping (8) can be written as

$$\boldsymbol{R} = \varrho\, \mathbf{C}(\Omega, i, \omega) \begin{pmatrix} \cos f \\ \sin f \\ 0 \end{pmatrix} \quad \text{and} \quad \dot{\boldsymbol{R}} = \sqrt{\frac{\mu}{p}}\, \mathbf{C}(\Omega, i, \omega) \begin{pmatrix} -\sin f \\ e + \cos f \\ 0 \end{pmatrix} \tag{24}$$

where

$$\varrho = \frac{p}{1 + e\cos f}\ , \qquad p = a\big(1 - e^2\big)\ , \qquad \text{and} \qquad f = f(M, e) \tag{25}$$

and

$$\mathbf{C}(\Omega, i, \omega) = \mathbf{C}_3(-\Omega)\mathbf{C}_1(-i)\mathbf{C}_3(-\omega) \tag{26}$$

with $\mathbf{C}_i$ being the single-axis rotation matrix for the i^{th} coordinate axis. While we are expressing position and velocity in terms of true anomaly angle f, differences in mean anomaly M are used to express the relative motion, therefore $f = f(M, e)$. Let $\tilde{}$ denote states of the OECM location

$$\tilde{\boldsymbol{X}} \triangleq \boldsymbol{\Gamma}(\tilde{\boldsymbol{\alpha e}}) \tag{27}$$

The Cartesian formation center of mass (CCM) state vector $\boldsymbol{X}^*$ is then expressed as

$$\boldsymbol{X}^* \triangleq \frac{1}{M} \sum_{i=1}^{N} m_i\, \boldsymbol{\Gamma}(\tilde{\boldsymbol{\alpha e}} + \delta\boldsymbol{\alpha e}_i) \tag{28}$$

Varying only one of the orbital elements at a time, the center of mass error vector becomes

$$\begin{aligned}\Delta\boldsymbol{X} &\triangleq \boldsymbol{X}^* - \tilde{\boldsymbol{X}} \\ &= \frac{1}{M}\sum_{i=1}^{N} m_i \left[\boldsymbol{\Gamma}(\tilde{\boldsymbol{oe}}) + \left.\frac{\partial \boldsymbol{\Gamma}}{\partial \tilde{oe}_i}\right|_{\text{OECM}} \delta oe_i + \frac{1}{2}\left.\frac{\partial^2 \boldsymbol{\Gamma}}{\partial \tilde{oe}_i^2}\right|_{\text{OECM}} \delta oe_i^2 + \mathcal{O}\big(\delta oe_i^3\big)\right] - \boldsymbol{\Gamma}(\tilde{\boldsymbol{oe}}) \\ &= \frac{1}{2M}\frac{\partial^2 \boldsymbol{\Gamma}}{\partial \tilde{oe}_i^2}\sum_{i=1}^{N} m_i\, \delta oe_i^2 + \mathcal{O}\big(\delta oe_i^3\big)\end{aligned} \tag{29}$$

Using similar arguments as were used to derive Eq. (22) first-order terms in the Taylor series expansion in Eq. (29) again vanish according to conditions (11). Let us investigate center of mass model deviations behavior further. Using Eq. (29) it is straightforward to show that with $\Delta\boldsymbol{X} = (\Delta\boldsymbol{R}, \Delta\dot{\boldsymbol{R}})$

$$\Delta\boldsymbol{R} = \frac{1}{M}\sum_{i=1}^{N} m_i \left(\sum_{k=2}^{\infty} \frac{1}{k!}\left.\frac{\partial^k \boldsymbol{R}}{\partial oe_i^k}\right|_{\text{OECM}} \delta oe_i^k\right) = \frac{1}{M}\sum_{k=2}^{\infty}\frac{1}{k!}\left.\frac{\partial^k \boldsymbol{R}}{\partial oe^k}\right|_{\text{OECM}} \left(\sum_{i=1}^{N} m_i\, \delta oe_i^k\right) \tag{30}$$

and therefore

$$\begin{aligned}\Delta R = \|\Delta\boldsymbol{R}\| &= \frac{1}{M}\frac{1}{2}\left\|\left.\frac{\partial^2 \boldsymbol{R}}{\partial oe_i^2}\right|_{\text{OECM}}\right\| \sum_{i=1}^{N} m_i\, \delta oe_i^2 + \mathcal{R}_{\Delta R}\big(\mathcal{O}(\delta oe_i^3)\big) \\ &= c_{\Delta R}\,\frac{1}{2M}\sum_{i=1}^{N} m_i\, \delta oe_i^2 + \mathcal{R}_{\Delta R}\big(\mathcal{O}(\delta oe_i^3)\big)\end{aligned} \tag{31}$$

where we have introduced the symbol $c_{\Delta R}$ to simplify notation. A similar expression is obtained for $\Delta\dot{R}$ *mutatis mutandis*; the root mean square (RMS) deviation ratio $\gamma(\delta oe_i)$ then yields

$$\gamma(\delta oe_i) \triangleq \frac{\Delta\dot{R}}{\Delta R} = \frac{c_{\Delta\dot{R}}}{c_{\Delta R}}\,\frac{\Big[1 + \tilde{\mathcal{R}}_{\Delta\dot{R}}\big(\mathcal{O}(\delta oe_i)\big)\Big]}{\Big[1 + \tilde{\mathcal{R}}_{\Delta R}\big(\mathcal{O}(\delta oe_i)\big)\Big]} = c\,(1 + \mathcal{O}(\delta oe_i)) \tag{32}$$

Algebraic expressions for RMS deviation approximation constants $c_{\Delta R} = c_{\Delta R}(\boldsymbol{oe}, \delta oe_i)$ and $c_{\Delta\dot{R}} = c_{\Delta\dot{R}}(\boldsymbol{oe}, \delta oe_i)$ are listed in the Appendix.

As discussed in a previous section, both the Cartesian and the orbital element description provide a meaningful definition for the system center of mass. While traditionally the CCM has been used extensively in the literature, the OECM offers distinct advantages for formation control applications. From this point of view it is more adequate to refer to the difference between the two center of mass definitions as *deviations* rather than errors. Consequently, we employ from now on the terminology *center of mass* (or equivalently *center of mass*) *deviation vector* to denote $\Delta\boldsymbol{X}$ and similarly $\Delta\boldsymbol{R}$ and $\Delta\dot{\boldsymbol{R}}$.

Reference [16] presents RMS deviations for a linearized relative motion description using orbital element differences which can be explained analytically using Eq. (29). The RMS deviations show a quadratic behavior in general with the exception of positional deviations due to variations in semi-major axis. In nonlinear mappings between orbit element and inertial Cartesian coordinates in Eq. (8), the satellite semi-major axes a_i appear linearly. Therefore, the position deviation vector yields $\Delta\boldsymbol{R}(\delta oe_i = \delta a_i) = \boldsymbol{0}$, as expected.

The following numerical simulation illustrates the formation center of mass model deviations.

The chief orbital element set is given in Table I. The individual orbit element differences are varied for each case shown up to a corresponding maximum satellites separation from the formation center of mass of 1000 meters.

Table I. Chief orbital elements.

Orbital element	a [km]	e [1]	i [°]	Ω [°]	ω [°]	M [°]
Value	6739.6	9.0×10^{-4}	51.7	14.6	-33.0	-19.0

Figure 2 shows parametric plots for $\Delta\dot{R}$ and ΔR as orbit element differences are increased. Ten steps are used to sweep the orbit element differences. Note the near-linear behavior plotting $\Delta\dot{R}$ vs. ΔR and predicted by Eq. (32) for the full nonlinear solution.

With RMS deviation approximation constants readily available (Appendix) we introduce the quantities $\epsilon(\Delta\dot{R})$ and $\epsilon(\Delta R)$ to measure the accuracy of RMS deviation approximations via

$$\epsilon(\Delta R) = \frac{\Delta R - c_{\Delta R}\,\frac{1}{2M}\sum_{i=1}^{N} m_i\,\delta\mathcal{Oe}_i^2}{\Delta R} = \frac{\mathcal{R}_{\Delta R}\big(\mathcal{O}(\delta\mathcal{oe}_i^3)\big)}{\Delta R}\,,\ \epsilon(\Delta\dot{R}) = \frac{\mathcal{R}_{\Delta\dot{R}}\big(\mathcal{O}(\delta\mathcal{oe}_i^3)\big)}{\Delta\dot{R}} \tag{33}$$

For the two-spacecraft formation example, Table II lists RMS position and velocity deviations and corresponding relative errors $\epsilon(\Delta R)$ and $\epsilon(\Delta\dot{R})$ for a spacecraft-center of mass displacement of 1000 m. The relative error magnitudes justify approximating center of mass deviations using only the first term in the expansion in Eq. (31).

Table II. Center of mass RMS deviations $\Delta\dot{R}$ and ΔR and relative errors of first-order center of mass RMS deviation approximations $\epsilon(\Delta\dot{R})$ and $\epsilon(\Delta R)$ for a formation of two spacecraft and a spacecraft-center of mass displacement of 1000 m.

$\delta\mathcal{oe}_i$	$\Delta\dot{R}$ [m/s]	$\epsilon\,(\Delta\dot{R})$ [%]	ΔR [m]	$\epsilon\,(\Delta R)$ [%]
δa_i	6.3545×10^{-5}	3.2974×10^{-7}	0	0
δe_i	2.7945×10^{-5}	5.3899×10^{-3}	5.5828×10^{-3}	2.0733×10^{-2}
δi_i	5.2028×10^{-5}	7.8786×10^{-7}	5.8517×10^{-2}	1.9257×10^{-7}
$\delta\Omega_i$	7.4239×10^{-5}	2.5434×10^{-7}	5.8184×10^{-2}	7.0776×10^{-8}
$\delta\omega_i$	8.4727×10^{-5}	5.2788×10^{-7}	7.4125×10^{-2}	1.5317×10^{-6}
δM_i	8.4791×10^{-5}	1.9782×10^{-7}	7.4181×10^{-2}	3.3985×10^{-8}

5.2. Second Order Momentum Expression

We pointed out before that for small relative spacecraft distances the total inertial angular momentum can be approximated reasonably well by the inertial angular momentum of the OECM, that is, $\boldsymbol{H}_{\text{OECM}} \approx \boldsymbol{H}$. In fact, using a Taylor series expansion about the OECM we found that $\boldsymbol{H}_{\text{OECM}}$ is a second-order accurate approximation of $\boldsymbol{H}$. We also note that the angular momentum expression in Eq. (21) is neither a function of ω nor M_0 (only the orbit geometry defines the angular momentum).

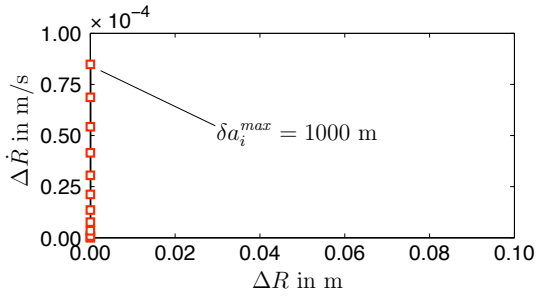

(a) C.M. error for varying δa_i

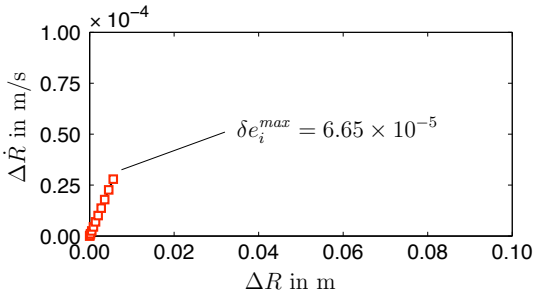

(b) C.M. error for varying δe_i

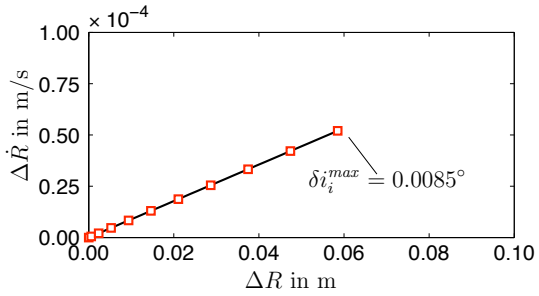

(c) C.M. error for varying δi_i

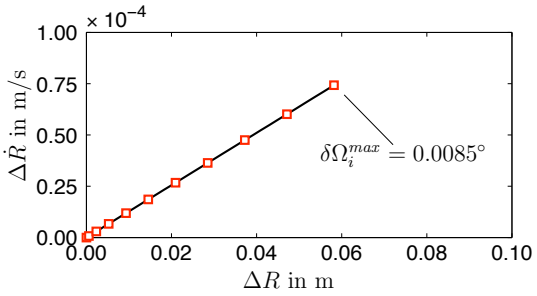

(d) C.M. error for varying $\delta\Omega_i$

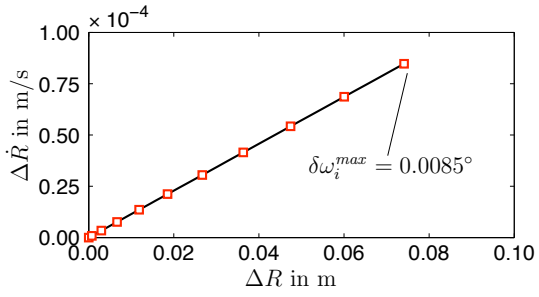

(e) C.M. error for varying $\delta\omega_i$

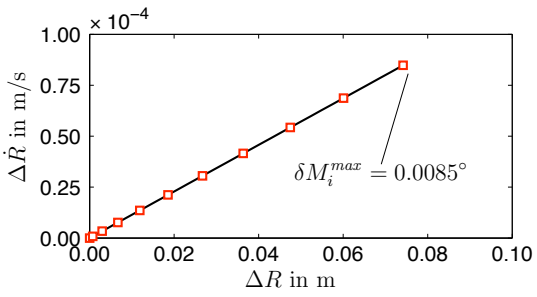

(f) C.M. error for varying δM_i

Figure 2. Center of mass RMS deviations $\Delta\dot{R}$ versus ΔR for a formation of two spacecraft and a maximal spacecraft-center of mass displacement of 1000 m using the full nonlinear solution. Discrete data points ▫ are plotted using equidistant step sizes $\delta\text{œ}_i$.

Hence, the "small" relative spacecraft separation assumption does not need to be satisfied in terms of these orbital elements for $\boldsymbol{H}_{\text{OECM}} \approx \boldsymbol{H}$ to hold.

Analyzing the dominating second-order terms in the expansion of $\boldsymbol{H}$ (Eq. (22)) we find that

$$\begin{aligned}\boldsymbol{H} = \boldsymbol{H}_{\text{OECM}} \left[1 + \sum_{i=1}^{N} \left(\frac{\delta a_i^2}{a_{\text{OECM}}} - \left(\delta\Omega_i^2 + \delta i_i^2\right)\right)\right] \; + \\ \left.\frac{\partial \boldsymbol{h}_i}{\partial a_i \partial \eta_i}\right|_{\text{OECM}} \sum_{i=1}^{N} m_i \delta a_i \delta\eta_i \; + \ldots + \; \mathcal{O}\big(\delta\boldsymbol{\alpha}_i^3, \delta\boldsymbol{\alpha}_i^2 \delta\boldsymbol{\alpha}_j, \ldots\big)\end{aligned} \tag{34}$$

It proves advantageous to use the eccentricity measure $\eta = \sqrt{1-e^2}$ rather than the eccentricity itself in the Taylor series expansion: η_i appear linearly in Eq. (21), therefore, there are no corresponding second-order terms in in the first line in Eq. (34). Nevertheless, the eccentricity does appear as a second-order effect through the mixed derivatives. Also, by using the eccentricity measure one can avoid mathematical singularities for cases when $e_i \to 1$, which would appear in the expansion otherwise.

In Eq. (34), the first group of terms such as $\partial^2 \boldsymbol{H}/\partial a_i^2$ produce deviations in the direction of $\boldsymbol{H}_{\text{OECM}}$ whereas the mixed second-order derivatives cause directional corrections to the angular momentum vector of the OECM. As indicated in the first line in Eq. (34), by dividing the entire equation through the common factor (at least in magnitude) of $|\boldsymbol{H}_{\text{OECM}}|$, we can compare second-order corrections directly to the leading term (which is $\boldsymbol{o}(1)$) and conveniently quantify deviations of the total angular momentum vector from $\boldsymbol{H}_{\text{OECM}}$.

6. Coulomb Control Influence on OECM

Consider the simple example of having N satellites floating in space in a "zero-gravity" environment. Because the Coulomb forces are formation internal forces, they cannot influence the motion formation Cartesian center of mass. However, if this same spacecraft cluster is orbiting about a planet, then the Coulomb forces can have an influence on the Cartesian center of mass motion. If the charges are used to slightly change the semi-major axis, then the satellites will drift apart and the CCM orbit radius will decrease. In contrast, it has already been shown that the OECM will evolve in a Keplerian manner if no spacecraft charges are active. In this section the spacecraft charge influence on the OECM is investigated. The question of interest is: can the OECM be approximated to be Keplerian even with spacecraft charges present?

For unperturbed and uncontrolled motion of the satellite formation the individual orbital elements of the satellites are constants of motion. Therefore, also the orbital elements of the OECM are constants of motion since, by definition, $\dot{\boldsymbol{\alpha}}_{\text{OECM}} = 1/M \sum_{i=1}^{N} m_i \dot{\boldsymbol{\alpha}}_i$. For controlled Coulomb formations, however, this is not the case. According to Gauss' variational equations the $\boldsymbol{\alpha}_i$ the time rate of change of orbital elements due to perturbing accelerations $\boldsymbol{u}_i$ can be written as [17]

$$\dot{\boldsymbol{\alpha}}_i = \mathbf{B}(\boldsymbol{\alpha}_i)\boldsymbol{u}_i \tag{35}$$

where $\mathbf{B}(\boldsymbol{\alpha}_i)$ is the 6×3 control influence matrix. For Coulomb formations the time rate of change

of the OECM therefore results in

$$\dot{\boldsymbol{oe}}_{\text{OECM}} = \frac{1}{M}\sum_{i=1}^{N} m_i \dot{\boldsymbol{oe}}_i = \frac{1}{M}\sum_{i=1}^{N} m_i \mathbf{B}(\boldsymbol{oe}_i)\boldsymbol{u}_i \tag{36}$$

where

$$\boldsymbol{u}_i = k_c \sum_{j\neq i}^{N} \frac{1}{m_i}\frac{q_i q_j}{|\boldsymbol{r}_{ij}|^3}\boldsymbol{r}_{ij} \tag{37}$$

In Eq. (36) the parameter $k_c = 8.99\times 10^9$ Nm^2/C^2 is Coulomb's constant, q_i is the (control) charge of the ith spacecraft and $\boldsymbol{r}_{ij}$ is the relative position vector of the jth spacecraft with respect to the ith spacecraft. Expanding the control influence matrix into a Taylor series about the OECM we find that

$$\dot{\boldsymbol{oe}}_{\text{OECM}} = \frac{1}{M}\left\{\mathbf{B}(\boldsymbol{oe}_{\text{OECM}})\sum_{i=1}^{N} m_i\boldsymbol{u}_i + \left[\!\!\left[\frac{\partial \mathbf{B}(\boldsymbol{oe})}{\partial \boldsymbol{oe}}\right]\!\!\right]\Big|_{\text{OECM}} \sum_{i=1}^{N} m_i \delta\boldsymbol{oe}_i \otimes \boldsymbol{u}_i + \mathcal{O}\big(\delta oe_i^2\big)\right\} \tag{38}$$

In Eq. (38) we have introduced the $\otimes$ operation to denote the multiplication of two n-vectors with a $n\times n\times n$ matrix. Note that Coulomb forces are system internal control forces. As a result the first term on the right-hand side of Eq. (38) vanishes. What we are left with is a dominating term proportional to expression of the form $\propto \delta\boldsymbol{oe}_i \otimes \boldsymbol{u}_i$. In other words

$$\dot{\boldsymbol{oe}}_{\text{OECM}} = \frac{1}{M}\left[\!\!\left[\frac{\partial \mathbf{B}(\boldsymbol{oe})}{\partial \boldsymbol{oe}}\right]\!\!\right]\Big|_{\text{OECM}} \sum_{i=1}^{N} m_i \delta\boldsymbol{oe}_i \otimes \boldsymbol{u}_i + \frac{1}{M}\,\mathcal{O}\big(\delta oe_i^2\big) = \mathcal{O}\big(\delta oe_i^2\big) \tag{39}$$

for $\boldsymbol{u}_i = \mathcal{O}\big(\delta\boldsymbol{oe}_i\big)$. Assume that the desired formation is prescribed through an orbit element difference set $\delta\boldsymbol{oe}_p$. Orbit element difference-based tracking error descriptions are then defined as $\Delta\boldsymbol{oe} = \delta\boldsymbol{oe} - \delta\boldsymbol{oe}_p$. The analysis in reference [7] demonstrates that for certain cases conventional control laws $\boldsymbol{u} \propto \mathbf{M}\,\Delta\boldsymbol{oe}$ based on Lyapunov's first method globally stabilize Coulomb formations. Typically we find that $\Delta\boldsymbol{oe} \ll \delta\boldsymbol{oe}$. However, even for the large tracking error case where $\Delta\boldsymbol{oe} \propto \delta\boldsymbol{oe}$, the third term in Eq. (39) is a second-order term. Thus the OECM motion can be considered to remain Keplerian to first order, as long as the charge control yields a control vector $\boldsymbol{u}_i$ which is at worst proportional to $\delta\boldsymbol{oe}_i$. A practical conclusion is that Coulomb formation control strategies using orbit element differences with respect to the OECM can assume that the OECM will continue a Keplerian motion (thus $\boldsymbol{oe}_{\text{OECM}} = \text{const.}$ and $\dot{\boldsymbol{oe}}_{\text{OECM}} = 0$) even while small spacecraft charging is present.

7. Conclusion

First order constraints of Coulomb formations are presented using orbit element differences. The formation chief position is chosen to be the formation center of mass. Because all Coulomb propulsion forces are formation internal forces, the inertial momentum vector of the entire formation is conserved. This constant vector, along with the center of mass definition of the formation chief, impose 6 constraints on the Coulomb formation. Using orbit element differences, first order approximations of the Cartesian center of mass are found. Further, the orbit element center of mass of the formation is introduced. This center of mass definition has advantages if used as a referenced point for formation control laws. The momentum constraint does not yield first order orbit element

constraint conditions. A careful analysis is presented detailing the position and velocity differences between the Cartesian and orbit element center of mass definitions. First order analytical solutions are presented to compute the center of mass differences. Further, this paper demonstrates that the OECM motion can be assumed to be Keplerian to first order, even while Coulomb charge control laws are active.

References

[1] Lyon B. King, Gordon G. Parker, Satwik Deshmukh, and Jer-Hong Chong. Spacecraft formation-flying using inter-vehicle coulomb forces. Technical report, NASA/NIAC, January 2002. `http://www.niac.usra.edu`.

[2] E. G. Mullen, M. S. Gussenhoven, and D. A Hardy. Scatha survey of high-voltage spacecraft charging in sunlight. *Journal of the Geophysical Sciences*, 91:1074–1090, 1986.

[3] K. Torkar, W. Riedler, C. P. Escoubet, M. Fehringer, R. Schmidt, R. J. L. Grard, H. Arends, F. Rüdenauer, W. Steiger, B. T. Narheim, K. Svenes, R. Torbert, M. André, A. Fazakerley, R. Goldstein, R. C. Olsen, A. Pedersen, E. Whipple, and H. Zhao. Active spacecraft potential control for cluster – implementation and first results. *Annales Geophysicae*, 19:1289–1302, 2001.

[4] Dwight R. Nicholson. *Introduction to Plasma Theory*. Krieger Publishing, Melbourne, FL 32902-9542, USA, 1992.

[5] Tamas I. Gombosi. *Physics of the Space Environment*. Cambridge University Press, The Edinburgh Building, Cambridge CB2 2RU, UK. New York, NY 10011-4211, USA, 1998.

[6] Lyon B. King, Gordon G. Parker, Satwik Deshmukh, and Jer-Hong Chong. Study of inter-spacecraft coulomb forces and implications for formation flying. *AIAA Journal of Propulsion and Power*, 19(3):497–505, May–June 2003.

[7] Hanspeter Schaub, Gordon G. Parker, and Lyon B. King. Challenges and prospect of coulomb formations. *Journal of the Astronautical Sciences*, 52(1–2):169–193, January–June 2004.

[8] Hanspeter Schaub. Stabilization of satellite motion relative to a coulomb spacecraft formation. *Journal of Guidance, Control, and Dynamics*, 28(6):1231–1239, November–December 2005.

[9] H. Joe, Hanspeter Schaub and Gordon G. Parker. Formation dynamics of coulomb satellites. In *6th International Conference on Dynamics and Control of Systems and Structures in Space*, Riomaggiore, Cinque Terre, Italy, July 2004, pp.79–90.

[10] Hanspeter Schaub and John L. Junkins. *Analytical Mechanics of Space Systems*. AIAA Education Series, AIAA Inc., Reston, VA 20191-4344, USA October, 2003.

[11] George William Hill. Researches in the lunar theory. *American Journal of Mathematics*, 1(1):5–26, 1878.

[12] W. H. Clohessy and R. S. Wiltshire. Terminal guidance system for satellite rendezvous. *Journal of the Aerospace Sciences*, 27(9):653–658, Sept. 1960.

[13] Hanspeter Schaub. Spacecraft relative orbit geometry description through orbit element differences. In *14th U.S. National Congress of Theoretical and Applied Mechanics*, Blacksburg, VA, June 2002.

[14] Hanspeter Schaub. Relative orbit geometry through classical orbit element differences. *Journal of Guidance, Control and Dynamics*, 27(5):839–848, Sept.–Oct. 2004.

[15] Hanspeter Schaub and Mischa Kim. Orbit element difference constraints for coulomb satellite formations. In *AIAA/AAS Astrodynamics Specialist Conference*, Providence, Rhode Island, Aug. 2004. Paper No. AIAA 04-5213.

[16] Hanspeter Schaub and Kyle T. Alfriend. Hybrid cartesian and orbit element feedback law for formation flying spacecraft. *Journal of Guidance, Control and Dynamics*, 25(2):387–393, March–April 2002.

[17] Richard H. Battin. *An Introduction to the Mathematics and Methods of Astrodynamics*. AIAA Education Series, AIAA Inc., Reston, VA 20191-4344, USA, 1987.

8. Appendix

In starting to analyze mappings (24), we notice that the coordinate transformations can be written as products $\mathbf{C}(\Omega, i, \omega)\,\boldsymbol{\xi}(a, e, f(M, e))$. Therefore, when evaluating derivatives with respect to a particular orbital element one needs to focus only on either the rotation matrix or the respective vector $\boldsymbol{\xi}$. We further note that for our analysis the true anomaly is treated as a dependent variable, depending on independent variables M and e.

Calculations of deviation constants $c_{\Delta\dot{R}}$ and $c_{\Delta R}$ for semimajor axis variations are straightforward. Deviation constant computations for variations in orbit orientation parameters $\{\Omega, i, \omega\}$ are facilitated by hand by using Singular Value Decompositions (SVD) for the particular rotation matrix. Note that

$$\frac{d^2}{d\alpha^2}\mathbf{C}_j(\alpha) = \mathbf{U}(\alpha)_j\mathbf{S}_j\mathbf{V}_j\ , \qquad j = 1, 2, 3 \tag{40}$$

where $|\det(\mathbf{U}_j)| = 1$, $\mathbf{S}_j$ projects vectors onto the 1–2 plane and $\mathbf{V}_j$ essentially simply reorders vector components. For the inclination angle, for example, the problem of calculating $(d^2/di^2)\,\mathbf{C}(\Omega, i, \omega)$ can therefore be replaced by the problem of computing $\mathbf{S}_1\mathbf{V}_1\mathbf{C}_3(-\omega)$. A similar analysis can be performed to yield deviation constants for the ascending node angle and the argument of periapses.

Deviation constants for mean anomaly variations and eccentricity variations are more complex since mappings (24) are expressed using true anomaly and $f = f(M, e)$ as pointed out before. For eccentricity variations $c_{\Delta\dot{R}}$ and $c_{\Delta R}$ are therefore calculated (using operator notation) $[d/de]^2\,(\cdot) \doteq \big[\partial/\partial e + (\partial f/\partial e)(\partial/\partial f)\big]^2(\cdot)$. Deviation constants for mean anomaly variations are obtained in a similar fashion.

Table III. First-order center of mass RMS deviation constants $c_{\Delta\dot{R}}$ and $c_{\Delta R}$.

$$\left\| \left. \frac{\partial^2 \dot{\boldsymbol{R}}}{\partial a_i^2} \right|_{\text{OECM}} \right\| = \sqrt{\frac{\mu}{p}} \frac{3}{4a^2} \sqrt{1 + 2e\cos f + e^2} \tag{41}$$

$$\left\| \left. \frac{\partial^2 \dot{\boldsymbol{R}}}{\partial e_i^2} \right|_{\text{OECM}} \right\| = \sqrt{\frac{\mu}{p}} \frac{1}{16(1-e^2)^2} \left\{ \Big[-20\,e + 2\big(-10 + 9\,e^2\big)\cos f + 48\,e\cos(2f) + \big(36 + 11\,e^2\big)\cos(3f) + 20\,e\cos(4f) + 3\,e^2\cos(5f) \Big]^2 + 4\Big[12 + 29\,e^2 + 76\,e\cos f + 4\big(9 + 4\,e^2\big)\cos(2f) + 20\,e\cos(3f) + 3\,e^2\cos(4f) \Big]^2 \sin^2 f \right\}^{1/2} \tag{42}$$

$$\left\| \left. \frac{\partial^2 \dot{\boldsymbol{R}}}{\partial i_i^2} \right|_{\text{OECM}} \right\| = \sqrt{\frac{\mu}{p}} \left| \cos(\omega + f) + e\cos\omega \right| \tag{43}$$

$$\left\| \left. \frac{\partial^2 \dot{\boldsymbol{R}}}{\partial \Omega_i^2} \right|_{\text{OECM}} \right\| = \sqrt{\frac{\mu}{p}} \sqrt{1 + 2e\cos f + e^2 - \sin^2 i \left[e\cos\omega + \cos(\omega + f) \right]^2} \tag{44}$$

$$\left\| \left. \frac{\partial^2 \dot{\boldsymbol{R}}}{\partial \omega_i^2} \right|_{\text{OECM}} \right\| = \sqrt{\frac{\mu}{p}} \sqrt{1 + 2e\cos f + e^2} \tag{45}$$

$$\left\| \left. \frac{\partial^2 \dot{\boldsymbol{R}}}{\partial M_i^2} \right|_{\text{OECM}} \right\| = \sqrt{\frac{\mu}{p}} \frac{(1 + e\cos f)^3}{(1-e^2)^3} \sqrt{\frac{2 + 4e\cos f + 5e^2 - 3e^2\cos(2f)}{2}} \tag{46}$$

$$\left\| \left. \frac{\partial^2 \boldsymbol{R}}{\partial a_i^2} \right|_{\text{OECM}} \right\| = 0 \tag{47}$$

$$\left\| \left. \frac{\partial^2 \boldsymbol{R}}{\partial e_i^2} \right|_{\text{OECM}} \right\| = \frac{p}{(1 + e\cos f)} \frac{|\sin f|}{\sqrt{8}(1-e^2)} \times \sqrt{20 - 12\cos(2f) + 8e\left[5\cos f - \cos(3f)\right] + e^2[33 - \cos(4f)]} \tag{48}$$

$$\left\| \left. \frac{\partial^2 \boldsymbol{R}}{\partial i_i^2} \right|_{\text{OECM}} \right\| = \frac{p}{1 + e\cos f} \left| \sin(\omega + f) \right| \tag{49}$$

$$\left\| \left. \frac{\partial^2 \boldsymbol{R}}{\partial \Omega_i^2} \right|_{\text{OECM}} \right\| = \frac{p}{1 + e\cos f} \sqrt{1 - \sin^2 i \sin^2(\omega + f)} \tag{50}$$

$$\left\| \left. \frac{\partial^2 \boldsymbol{R}}{\partial \omega_i^2} \right|_{\text{OECM}} \right\| = \frac{p}{1 + e\cos f} \tag{51}$$

$$\left\| \left. \frac{\partial^2 \boldsymbol{R}}{\partial M_i^2} \right|_{\text{OECM}} \right\| = \frac{a\,(1 + e\cos f)^2}{(1-e^2)^2} \tag{52}$$